Journal of Volcanology and Geothermal Research 94 (2010) 214–219

Contents lists available at ScienceDirect

Journal of Volcanology and Geothermal Research

journal homepage: www.elsevier.com/locate/jvolgeores

Short communication

Heat transfer coefficients of natural volcanic clasts

Tom Wylie Stroberg [a], Michael Manga [a,*], Josef Dufek [b]

[a] Earth and Planetary Science, University of California, Berkeley, Berkeley CA 94720-4767, United States
[b] School of Earth and Atmospheric Sciences, Georgia Institute of Technology, Atlanta, GA, United States

ARTICLE INFO

Article history:
Received 5 February 2010
Accepted 13 May 2010
Available online 27 May 2010

Keywords:
pumice
heat transfer coefficients
permeability

ABSTRACT

Heat transfer coefficients used in numerical simulations of volcanic eruptions are typically borrowed from industrial settings where the coefficients are well determined for non-permeable, machined (spherical) materials. Volcanic clasts, in contrast, are permeable and have irregular shapes. We performed a series of laboratory experiments to determine heat transfer coefficients for natural volcanic particles. We measured the surface and interior temperatures during cooling at wind speeds ranging from 0 to 10 m/s. We also measured the permeability and density of the particles. We find that the permeability of the particles has little effect on clast cooling. In the absence of any wind, heat loss occurs by free convection, and we find no relationship between the heat transfer coefficient and particle density. However, for non-zero Reynolds numbers (finite wind speed), the heat transfer coefficient decreases with increasing porosity. We obtain a correlation for the dimensionless heat loss, or Nusselt number, of the form $Nu = 2 + a\mathrm{Re}^{1/2}\mathrm{Pr}^{1/3}$ where a is a density dependent coefficient given by $a = 0.00022\rho + 0.31$, with ρ in kg/m^3, and Re and Pr are the Reynolds number and Prandtl number, respectively. Compared with non-porous particles, heat transfer coefficients for natural pumice clasts are reduced by a factor of 2–3 for particles with similar Re. Numerical simulations show that this leads to an increase in depositional temperature by 50–90 °C.

1. Introduction

Heat transfer from particles to the surrounding gas during explosive volcanic eruptions affects the buoyancy of the gas–particle mixture and the gas pressure (e.g., Woods and Bursik, 1991). Thus the rate of heat transfer can influence the runout of pyroclastic density currents and elutriation of fine ash. The time scale over which particles cool also affects their degassing (Hort and Gardner, 2000), oxidation (Tait et al., 1998), expansion and quenching (Kaminski and Jaupart, 1997). For these reasons, numerical simulations of pyroclastic density currents and explosive eruptions often include models for particle–gas heat transfer (e.g., Dobran et al., 1993; Neri and Macedonio, 1996; Dartevelle et al., 2004; Dufek and Bergantz, 2007a).

Heat transfer properties are typically characterized by a so-called "heat transfer coefficient", and are usually measured for spherical, non-porous particles (e.g., Mallory, 1969; Touloukian and Ho, 1972). In contrast, natural volcanic particles are irregular in shape and porous. Particle shape can alter heat transfer coefficients by changing the properties of the thermal boundary layer around particles across which heat is conducted. Porous particles may also alter heat transfer coefficients by allowing increased airflow through the particle pores, thereby expediting cooling.

Here we performed a series of laboratory experiments to determine the sensitivity of volcanic particle heat transfer coefficients to variations of permeability and density. We find values that can differ by factors exceeding 3 compared with standard engineering values for spherical particles. We also present an example numerical simulation in which we assess the role of error or uncertainty in the heat transfer coefficient on the depositional temperature of centimeter-sized clasts.

2. Samples

We measured heat transfer coefficients for a range of natural volcanic particles to encompass different densities and permeabilities. We also made the same measurements on glass spheres in order to compare our results with well-established literature values (e.g., Whitaker, 1972).

The volcanic samples are air fall from the ~850 BP Glass Mountain eruption at Medicine Lake volcano, California (numbered samples), and basaltic scoria from Coso, California (Scoria 1 and 2). Sample properties are summarized in Table 1 and photographs of particles are shown in Fig. 1.

3. Methods

Heat transfer coefficients were measured by recording the cooling rates of the particles shown in Fig. 1 and listed in Table 1. A 1 mm diameter thermocouple wire was inserted into a 1 mm diameter hole drilled into

* Corresponding author. Tel.: +1 510 643 8532.
E-mail address: manga@seismo.berkeley.edu (M. Manga).

0377-0273/$ – see front matter © 2010 Elsevier B.V. All rights reserved.
doi:10.1016/j.jvolgeores.2010.05.007

Table 1
Properties of volcanic clasts and glass beads.

Sample	Density (kg/m^3)	c_p (J/kg K)	r_c (m)	$K\times10^{14}$ (m^2)
1	830	826	0.00895	2.17
2	593	815	0.00782	1.78
3	846	817	0.00895	1.29
6	1,450	853	0.00755	<0.02
7	982	826	0.00874	1.49
11	720	835	0.00914	0.05
14	726	851	0.00831	1.06
16	1,290	835	0.00620	0.05
20	1,500	859	0.00807	<0.02
21	1,630	856	0.00807	<0.02
22	2,510	834	0.00659	<0.02
Scoria 1	709	865	0.00853	8.54
Scoria 2	685	860	0.00895	107
Glass bead	2,390	818	0.00805	<0.02

the interior of each sample. We heated samples to 200 °C in a convection oven. Once the internal temperature reading from the thermocouple was steady, we removed the sample from the oven and recorded its cooling. We monitor internal temperature with the thermocouple and the surface temperature with an infrared camera (FLIR A3280). We report average surface temperatures using factory calibration. Sampling rate was 1 s^{-1} for both temperature measurements.

To simulate the motion of the particles relative to the gas phase, we used a fan to produce different wind speeds and held the particles fixed in space in a wire cage. For each particle, temperature measurements were recorded at four wind speeds ranging from 0 to 10 m/s. To measure the velocity of the airflow past the particle, a velocimeter was placed on the wire stand used to hold the particle prior to the particle being removed from the oven. The fan was turned on and the wind speed was recorded and averaged over a period of 30 s. The velocimeter was then removed so as not to interfere with the flow past the particle. Temperature measurements were recorded for 200–500 s, depending on the observed cooling.

The heat transfer coefficient, H, is defined from

$$q = HA_s(T-T_\infty),$$

where q is the heat flow from the particle, A_s is the particle surface area, T is the mean particle temperature in °C, and T_∞ is the ambient temperature. To calculate H from our temperature measurements, we assume a lumped capacitance model (e.g., Incropera et al., 2006) so that the heat transfer coefficient can be calculated from

$$H = -\frac{\rho c_p V}{A_s t}\ln\left(\frac{T-T_\infty}{T_i-T_\infty}\right) \quad (1)$$

where ρ is the density of the particle, c_p is the specific heat, V is the volume, t is time, and T_i is the initial temperature. The lumped capacitance model assumes that the particle temperature is close to uniform and that cooling is limited by heat loss from the particle surface.

The lumped capacitance model is strictly valid for Biot numbers

$$Bi = \frac{Hr_c}{k_p} \ll 1 \quad (2)$$

where r_c is a characteristic particle dimension, and k_p is the thermal conductivity of the particle. This dimensionless group can be interpreted as the ratio of the boundary layer thermal resistance to the internal thermal resistance of the solid. In our experiments, Bi

Fig. 1. Particles for which we measured heat transfer coefficients. Properties are listed in Table 1. In some particles, the hole into which the thermocouple was placed can be seen.

ranged from 0.1 to more than 10. However, our temperature measurements fit Eq. (1) well for all experiments and thus the lumped capacitance model was still used to obtain H. The measured surface temperature and interior temperature differed by less than a few degrees at the sampling interval of 1 s, providing further justification for the uniform temperature approximation. When Bi is not $\ll 1$, H is also influenced by the thermal conductivity of the particle.

The particle size r_c is not well defined for irregular-shaped particles. We thus define a characteristic length and surface area as

$$r_c = \left(\frac{3}{4\pi}V\right)^{\frac{1}{3}} \tag{2a}$$

$$A_s = \pi r_c^2 \tag{2b}$$

where V is the measured volume of the particle.

An estimate of permeability is important to assess the possible contribution of gas flowing through the particle on the heat transfer. Permeability of individual clasts is not the most meaningful quantity, nor is it straightforward to measure, as it is likely anisotropic (Degruyter et al., 2009; Wright et al., 2009). Moreover, in most cases the airflow is dominated by one or a small number of flow paths. Nevertheless, it is useful to have an estimate of the property. To obtain a measurement of permeability, we modified the constant head gas permeameter developed in Saar and Manga (1999). Since the samples had naturally occurring geometries, simple permeameters designed for use with cylindrical samples could not be used. Instead, we sealed the particles into the end of a PVC tube using paraffin wax and forced air through the tube and particle. We measured the flow rate into the tube and the pressure inside the tube. To determine the permeability, K, we used the solution to the one-dimensional gas flow equation for an ideal, compressible fluid (e.g., Dullien, 1992):

$$K = \frac{2\mu Q p_1 L}{A(p_1^2 - p_o^2)} \tag{3}$$

where μ is the gas viscosity, Q is the gas flux, p_1 is the inlet pressure, p_o is the outlet pressure which is equal to the atmospheric pressure, L is the distance across which the pressure drop occurs, and A is the cross sectional area of the sample. In the case of naturally occurring particles, both L and A are not well defined. As before, we therefore defined them as $L = r_c$ and $A = A_c$.

We measured density by recording the mass of the particles using an electronic scale then coating the samples in a thin layer of paraffin wax and submerging them in water to obtain an estimate of the volume. To determine the heat capacity of the volcanic samples, we used a temperature dependent relation presented in Dufek et al. (2007). Heat capacity of the glass sphere was measured using a styrofoam calorimeter. We placed a known volume of room temperature water in the calorimeter then inserted a known mass of glass beads at 160 °C. A thermocouple measured the temperature. Once the system reached an equilibrium temperature, and knowing the heat capacity of water, the heat capacity of the glass beads was determined through an energy balance.

We neglect the temperature-dependence of thermal conductivity and diffusivity as measurements show that it is small over the range of temperature we consider (e.g., Bagdassarov and Dingwell, 1994). Radiative heat transfer can also be neglected in our experiments (and in most natural pyroclasts) because radiative transfer only becomes important for temperatures above 800 °C (Keszthelyi, 1994) or even higher (e.g., Bagdassarov and Dingwell, 1994). Thus, while our data are collected for particles cooling at temperatures less than 200 °C, the results should be applicable for most volcanically-relevant conditions.

4. Results

Fig. 2 shows one example of the temperature measurements collected for a cooling particle. The data shown is for sample 22 subjected to a wind speed of 3.5 m/s with an ambient temperature of 25 °C. In order to characterize particle cooling, we calculate a dimensionless heat loss, or Nusselt number, defined as

$$Nu = \frac{2Hr_c}{k_{air}} \tag{4}$$

where the thermal conductivity of air k_{air} is 0.0257 $Wm^{-1}K^{-1}$. To calculate H, we calculated the best-fit line that relates the logarithmic temperature difference from Eq. (1) and time. The slope of this line is inversely proportional to the heat transfer coefficient, with the constant of proportionality consisting of known properties of the samples.

Fig. 3 compares measured Nu for the glass spheres with standard empirical correlations for spheres (e.g., Ranz and Marshall, 1952),

$$Nu = 2 + 0.6Re^{\frac{1}{2}}Pr^{\frac{1}{3}} \tag{5}$$

where Pr is the Prandtl number for air at room temperature. The Prandtl number is a dimensionless parameter relating the rate of momentum diffusion to thermal diffusion and is given by the ratio of kinematic viscosity to thermal diffusivity of the air. The Reynolds number, Re, relates inertial forces to viscous forces and is given by

$$Re = \frac{2ur_c}{\nu} \tag{6}$$

where u is the wind speed, r_c is the size of the sample, and ν is the kinematic viscosity of air. Over the range of Reynolds number (wind speeds) we were able to achieve, our measurements agree with the form of Eq. (1) for both Nu calculated from interior and surface temperatures. The agreement is slightly better when Nu is based on surface temperatures so we hereafter rely only on measured surface temperatures.

Fig. 4 shows measured Nu for all particles at all Re. At a given Re, Nu decreases as the particle density decreases. Over the range of parameters explored, heat transfer coefficients varied by more than a factor of 10: from 15 $Wm^{-2}K^{-1}$ for a low density, porous particle with no forced convection to 144 $Wm^{-2}K^{-1}$ for an angular obsidian sample (particle 22) subjected to a wind speed of 10 m/s.

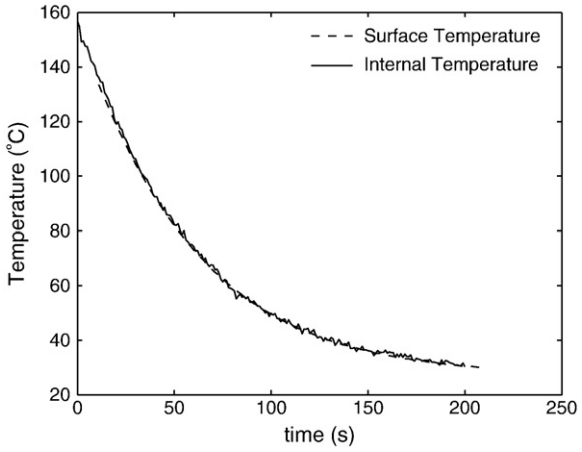

Fig. 2. Surface and internal temperature as a function of time, measured with an infrared camera and thermocouple respectively, for particle 22 (see Fig. 1 and Table 1), wind speed 3.5 m/s, and ambient temperature 25 °C.

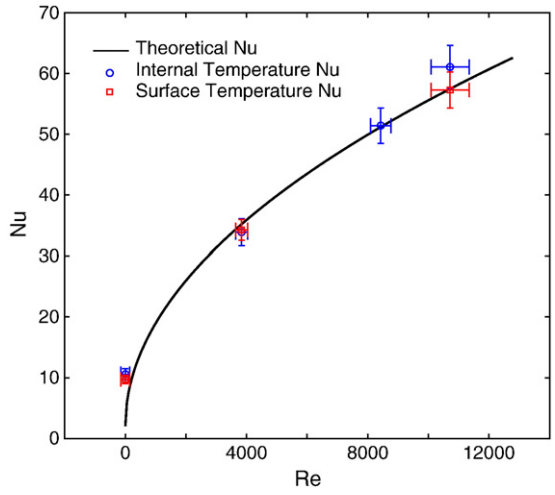

Fig. 3. Comparison of measured Nusselt numbers, Nu, for a glass sphere with standard empirical correlations (Ranz and Marshall, 1952). Although both the data from the thermocouple and infrared camera fit the correlation within the error bars, Nu obtained from the surface temperature appears to be a better match.

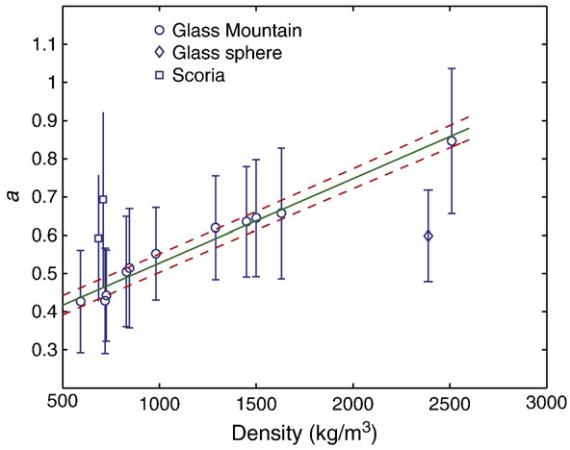

Fig. 5. Coefficient a, as defined in Eq. (7), to a fit similar to that proposed by Ranz and Marshall (1952) as a function of particle density. The best fit that relates a to density is given by the straight line with uncertainty shown by the dashed lines. Correlation coefficient for this linear relationship is 0.985. The two scoria samples, plotted with the squares, and the glass bead, plotted with the diamond, are not included in the fit.

For each particle, we calculated a correlation coefficient, a, relating the Nusselt number to the Reynolds number by an equation of the form

$$Nu = 2 + aRe^{\frac{1}{2}}Pr^{\frac{1}{3}} \tag{7}$$

where we retain the same functional dependence on Re and Pr as in Eq. (5). Fig. 5 shows a as a function of particle density ρ. A linear fit to the data in Fig. 5 gives $a = (2.2 \pm 0.3) \times 10^{-4}\rho + (0.31 \pm 0.04)$ with ρ in kg/m^3.

5. Discussion

In Fig. 4 we show model predictions given by Eq. (7) for the highest and lowest density natural clasts. Also shown is the equivalent relationship, Eq. (5), for spherical particles. There are two ways in which the heat transfer coefficients for natural clasts differ from those of the glass beads. First, for the non-porous particles, the heat transfer coefficient for natural clasts is higher than that for spherical particles owing to the increased surface area to volume ratio for non-spherical particles. Second, as the density of the clasts decreases, so too does the rate of heat transfer. The approximately linear dependence of H on density mirrors the effect of density on thermal conductivity k_p, at least for porosities over the range we have considered (e.g., Francl and Kingery, 1954; Jeffrey, 1973; Davis, 1986). Because H accounts for the effect of density on heat content, our measurements show that dense particles transfer heat faster to their surroundings than more porous clasts. While we could not measure the thermal conductivity of our clasts, the linear relationship between cooling rate and porosity indicates that heat loss is also influenced by the thermal conductivity of the particles.

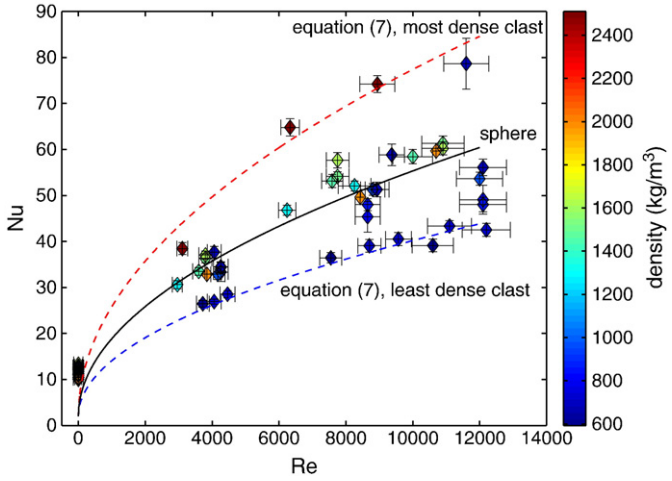

Fig. 4. Nu as a function of Re number for all particles. Solid curve is the Ranz and Marshall (1952) correlation for spherical particles given by Eq. (5). The red and blue dashed curves are predictions of Eq. (7) for the most and least dense clasts, respectively. The color of the symbols shows the density of the particle.

Fig. 5 shows that Eq. (7), in which heat transfer depends only on wind speed (via Re) and particle density (via a), provides a good fit to the measurements, with a correlation coefficient of 0.9850 for the Glass Mountain samples. The two scoria samples plot above this trend. These two samples also have the highest permeability, but, as discussed next, their permeability is still not large enough to enhance their cooling. Overall, permeability has no clear effect on heat transfer: the relationship between a and permeability k has a correlation coefficient of 0.5855, not statistically significant.

We can calculate an *upper* bound on the amount of heat removed by gas flowing through the porous particles. To do so, we first calculated the mass flow rate through the particle's pores using the highest permeability measured during the experiments. The mass flow rate is given by

$$\dot{m} = \rho_{air} Q, \tag{8}$$

where ρ_{air} is the density of the air at room temperature and Q is the volumetric flow rate found by rearranging Eq. (3). Although the uncertainty associated with the permeability measurements is large, the values obtained are of the same order of magnitude as those measured in previous studies of volcanic clast permeability (e.g., Klug and Cashman, 1996; Saar and Manga, 1999; Sruoga et al., 2004; Bernard et al., 2007). The pressure difference across the particle in Eq. (3) is taken to be the dynamic pressure at a stagnation point

$$p_1 - p_0 = \frac{1}{2}\rho_{air} u^2 \tag{9}$$

where u is the far field velocity and we use 200 m/s as a reasonable estimate of the upper limit of relative velocity. The rate of heat

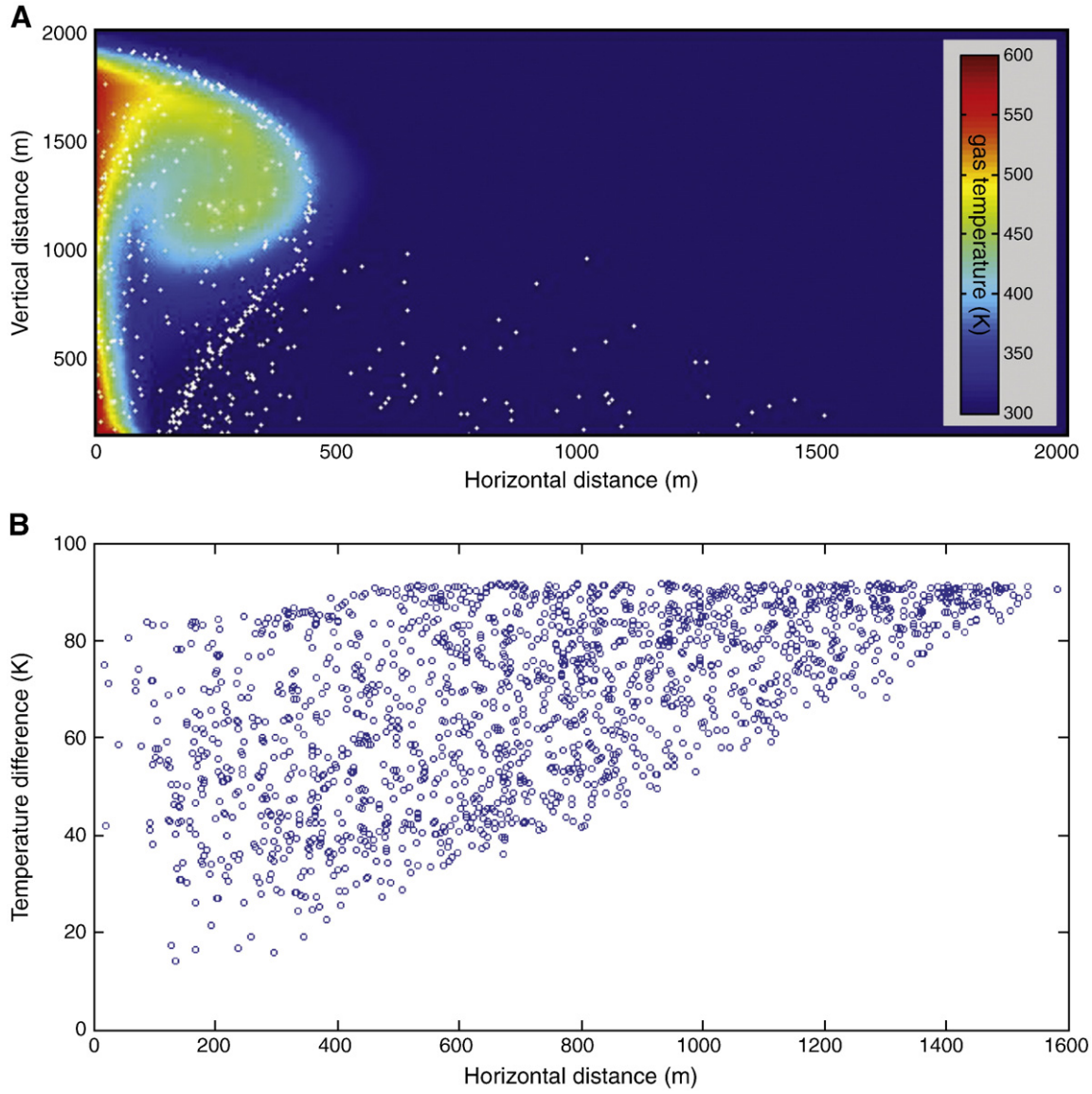

Fig. 6. A) An example numerical simulation of an explosive showing gas temperature (color) and location of Lagrangian tracer particles 80 s into eruption. Vent velocity is 200 m/s, vent temperature is 1000 K, particle concentration is 0.0005, particle size is 100 μm. Ballistic particles are introduced at the vent and are coupled to the surrounding gas and particles, as in Dufek et al. (2007). 50,000 ballistic particles, ranging in size from 1 to 50 cm, are seeded randomly at the vent during the first 50 s of the eruption. Vertical and horizontal axes are position in meters. B.) Difference in depositional temperature of 5 cm size particles if the heat transfer coefficient is that for pumice with density of 1040 kg/m^3 rather than for dense particles (2600 kg/m^3). A positive temperature anomaly indicates a warmer depositional temperature.

transfer and total energy transferred during cooling, assuming the gas equilibrates thermally with the particle, are estimated by

$$q = \dot{m} c_{p_{air}} \left(T_f - T_\infty\right)$$
$$E_{pore} = \int_0^\infty q dt = 4\dot{m} c_{p_{air}} (T_i - T_\infty) \rho c_p r_c / 3H \qquad (10a, b)$$

where $c_{p_{air}}$ is the specific heat of air at STP, T_f is the temperature of the air at the outlet of the pore, assumed to be equal to the temperature of the particle, and T_∞ is the temperature of the air at the inlet of the pore, assumed to be 30 °C. Substituting values into the above equations, and using our experimentally determined results for H, gives $E_{pore} \approx 2$ J for $K = 10^{-14}$ m^2, $\rho = 1000$ kg/m^3 and $r_c = 1$ cm. This is <1% of the thermal energy lost by a 2 g clast cooling from 200 °C, indicating that the effect of permeability on the heat transfer characteristics is expected to be negligible, as we found in our measurements. Note that even for the most permeable scoria particles, heat loss by flow through the particles will also be negligible under experimental conditions.

In order to assess whether the difference in heat transfer coefficients between spherical particles and natural clasts is significant, we present the results of one representative numerical simulation. We do not attempt a full study of all possible situations in which heat transfer plays a role, as our primary goal is to determine heat transfer coefficients that can be used broadly in numerical and theoretical models.

In the illustrative model problem we consider a low column explosive eruption. We choose properties so that we obtain a stable, buoyant and dilute column through which ballistic particles travel without the complication of an unsteady collapsing column and pyroclastic density currents. The numerical simulation used a coupled Eulerian–Eulerian formulation for the particle and gas phase (Dufek and Bergantz, 2007a) and treats larger particles as Lagrangian particles coupled to the flow (Dufek and Bergantz, 2007b). A mixture of 100 μm particles and gas erupts from a vent with velocity of 200 m/s. Particle concentration is 0.0005 so that conditions are choked at the vent. Vent temperature is 1000 K. Calculations are performed in a two-dimensional Cartesian geometry. Fig. 6A shows the distribution of temperature 80 s after the eruption is initiated. Into this eruption, 50,000 larger Lagrangian particles

are introduced. Lagrangian particles are influenced by the external flow and collisions with smaller particles, but do not, in turn, influence the large-scale dynamics. Lagrangian particles have diameters from 1 to 50 cm; their positions after 80 s are shown by the white dots. We monitor the temperature of these larger clasts and in particular their temperature upon deposition. The solid–gas heat transfer coefficients determined from the experiments along with the surface temperature of the clasts determine the heat flux from the clasts. The internal thermal profiles in the clasts are calculated assuming spherical conduction. Fig. 6B shows the difference between depositional temperature if we assume a heat transfer coefficient for pumice (density = 1040 kg/m^3) compared with dense clasts (density 2600 kg/m^3). The heat transfer coefficients we found for porous clasts result in average depositional temperatures that are typically 50–90 °C greater than the equivalent for non-porous clasts.

6. Conclusions

We measured heat transfer coefficients for natural volcanic clasts. We find that particle permeability has no significant effect but density matters for high wind speeds. Pumice particles cool about 3 times more slowly than their dense equivalents at wind speeds (relative velocity between particles and surrounding gas) of 10 m/s. We propose that Eqs. (7) be used in numerical simulations that include such heat transfer processes (e.g., Dobran et al., 1993; Neri and Macedonio, 1996; Dartevelle et al., 2004; Dufek and Bergantz, 2007a). The variability we find in our heat transfer coefficients can be thought of as an uncertainty or error that propagates through numerical simulations and analytical models into large-scale dynamics and depositional temperature. Without *a priori* knowledge of specific particle properties, the range of heat transfer coefficients we have found translates into a ~100 °C uncertainty in the depositional temperature of ballistic particles.

Acknowledgements

We thank the Berkeley Undergraduate Research Apprenticeship Program and NSF grants 0809564 (WS and MM) and 0809321 (JD) for support. Ameeta Patel helped with the lab measurements. We thank M. Hort and an anonymous reviewer for comments on the manuscript.

References

Bagdassarov, N., Dingwell, D., 1994. Thermal properties of vesicular rhyolite. J. Volcanol. Geotherm. Res. 60, 179–191.
Bernard, M.-L., Zamora, M., Geraud, Y., Boudon, G., 2007. Transport properties of pyroclastic rocks form Montagne Pelee volcano (Matinique, Lesser Antilles). J. Geophys. Res. 112, B05205.
Dartevelle, S., Rose, W.I., Stix, J., Kelfoun, K., Vallance, J.W., 2004. Numerical modeling of geophysical granular flows: 2. computer simulations of plinian clouds and pyroclastic flows and surges. Geochem. Geophys. Geosyst. 5, 1–36.
Davis, R.H., 1986. The effective thermal conductivity of a composite material with spherical inclusions. Int. J. Thermophys. 7 (3), 609–620.
Degruyter, W., Bachmann, O., Burgisser, A., 2009. Controls on magma permeability in the volcanic conduit during the climactic phase of the Kos Plateau Tuff eruption (Agean Arc). Bull. Volcanol. 72 (1), 63–74.
Dobran, F., Neri, A., Macedonio, G., 1993. Numerical simulation of collapsing volcanic columns. J. Geophys. Res. 98, 4231–4259.
Dufek, J., Bergantz, G.W., 2007a. The suspended-load and bed-load transport of particle laden gravity currents: insight from pyroclastic flows that traverse water. J. Theor. Comput. Fluid Dyn. 21, 119–145.
Dufek, J., Bergantz, G.W., 2007b. The dynamics and deposits generated by the Kos Plateau Tuff eruption: the controls on basal particle loss on pyroclastic flow transport. Geochem. Geophys. Geosyst. 8. doi:10.1029/2007GC001741.
Dufek, J., Manga, M., Staedter, M., 2007. Littoral blasts: pumice–water heat transfer and the conditions for steam explosions when pyroclastic flows enter the ocean. J. Geophys. Res. 112, B11201.
Dullien, F.A.L., 1992. Porous Media — Fluid Transport and Pore Structure, 2nd edition. Academic Press, San Diego, California. 574 pp.
Francl, J., Kingery, W.D., 1954. Experimental investigation on the effects of porosity on thermal conductivity. J. Am. Ceram. Soc. 37, 99–107.
Hort, M., Gardner, J., 2000. Constraints on cooling and degassing of pumice during Plinian volcanic eruptions based on model calculations. J. Geophys. Res. 105, 25,981–26,001.
Incropera, F.P., DeWitt, D.P., Bergman, T.L., Lavine, A.S., 2006. Fundamentals of Heat and Mass Transfer, 6th edition. John Wiley and Sons. 997 pp.
Jeffrey, D.J., 1973. Conduction through a random suspension of spheres. Proc. R. Soc. Lond. 335, 355–367.
Kaminski, E., Jaupart, C., 1997. Expansion and quenching of vesicular magma fragments in Plinian eruptions. J. Geophys. Res. 102, 12,187–12,203.
Keszthelyi, L., 1994. Calculated effect of vesicles on the thermal properties of cooling lava flows. J. Volcanol. Geotherm. Res. 63, 257–266.
Klug, C., Cashman, K.V., 1996. Permeability development in vesiculating magma. Bull. Volcanol. 58, 87–100.
Mallory, J.F., 1969. Thermal Insulation. Van Nostrand Reinhold, New York.
Neri, A., Macedonio, G., 1996. Numerical simulation of collapsing volcanic columns with particles of two sizes. J. Geophys. Res. 101, 8153–8174.
Ranz, W., Marshall, W., 1952. Evaporation from drops. Chem. Eng. Prog. 48, 141–146.
Saar, M.O., Manga, M., 1999. Permeability of vesicular basalts. Geophys. Res. Lett. 26, 111–114.
Sruoga, P., Rubinstein, N., Hinterwimmer, G., 2004. Porosity and permeability in volcanic rocks: a case study on the Serie Tobifera, South Patagonia, Argentina. J. Volcanol. Geotherm. Res. 132, 31–43.
Tait, S., Thomas, R., Gardner, J., Jaupart, C., 1998. Constraints on cooling rates and permeabilities of pumice in an explosive eruption jet from color and magnetic mineralogy. J. Volcanol. Geotherm. Res. 86, 79–91.
Touloukian, Y.S., Ho, C.Y. (Eds.), 1972. Thermophysical Properties of Matter. : Thermal Conductivity of Nonmetallic Solids, vol. 2. Plenum Press, New York.
Whitaker, S., 1972. Forced convection heat transfer correlations for flow in pipes, past flat plates, single cylinders, single spheres and flow in packed beds and tube bundles. Am. Inst. Chem. Eng. J. 18, 361–371.
Woods, A.W., Bursik, M.I., 1991. Particle fallout, thermal disequilibrium and volcanic plumes. Bull. Volcanol. 53, 559–570.
Wright, H.M.N., Cashman, K.V., Gottesfeld, E.H., Roberts, J.J., 2009. Pore structure of volcanic clasts: measurements of permeability and electrical conductivity. Earth Planet. Sci. Lett. 280, 93–104.